

Photocatalytic (Het)arylation of C(sp³)–H Bonds with Carbon Nitride

Saikat Das, Kathiravan Murugesan, Gonzalo J. Villegas Rodríguez, Jaspreet Kaur, Joshua P. Barham, Aleksandr Savateev, Markus Antonietti, and Burkhard König*

Cite This: *ACS Catal.* 2021, 11, 1593–1603

Read Online

ACCESS |



Metrics & More



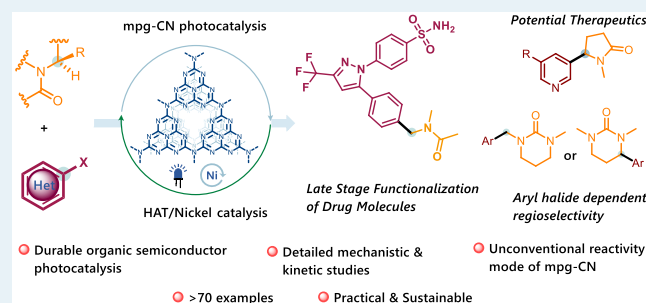
Article Recommendations



Supporting Information

ABSTRACT: Graphitic carbon nitride materials have attracted significant interest in recent years and found applications in diverse light-to-energy conversions such as artificial photosynthesis, CO₂ reduction, or degradation of organic pollutants. However, their utilization in synthetic photocatalysis, especially in the direct functionalization of C(sp³)–H bonds, remains underexplored. Herein, we report mesoporous graphitic carbon nitride (mpg-CN) as a heterogeneous organic semiconductor photocatalyst for direct arylation of C(sp³)–H bonds in combination with nickel catalysis. Our protocol has a broad synthetic scope (>70 examples including late-stage functionalization of drugs and agrochemicals), is operationally simple, and shows high chemo- and regioselectivities. Facile separation and recycling of the mpg-CN catalyst in combination with its low preparation cost, innate photochemical stability, and low toxicity are beneficial features overcoming typical shortcomings of homogeneous photocatalysis. Detailed mechanistic investigations and kinetic studies indicate that an unprecedented energy-transfer process (EnT) from the organic semiconductor to the nickel complex is operating.

KEYWORDS: heterogeneous photocatalysis, carbon nitride, hydrogen atom transfer, C(sp³)–H arylation, dual photo nickel, drug molecule functionalization



Over the past decade, the use of visible light has had a resurgence as an ideal reagent for catalytic synthetic transformations.^{1,2} A recent application of visible light photocatalysis is the direct functionalization of C(sp³)–H bonds. Since such bonds are the most abundant moiety in organic molecules, their direct activation allows for efficient chemical diversification avoiding prefunctionalization steps.^{3,4} Specially designed homogeneous catalysts such as transition-metal-based polypyridine complexes⁵ or organic dyes⁶ and in some cases inorganic semiconductors⁷ have been used for C–H bond functionalization. However, in practice, most solution-phase catalysts show limited durability; they are prone to deactivation in the presence of reactive radical intermediates^{6,8–10} or suffer from drastic changes to their photophysical properties upon changes in the pH of the reaction medium.¹¹ The selection of a photocatalyst for a given transformation therefore remains a challenge. In addition to catalyst instability, the nonrecyclability limits the practical use of many well-known homogeneous catalysts for direct functionalization of C–H bonds, particularly on a larger scale. Herein, we report the use of a heterogeneous organic semiconductor, mesoporous graphitic carbon nitride (mpg-CN), as a robust photocatalyst for direct arylations of C(sp³)–H bonds.

Graphitic carbon nitride, the most stable allotrope of carbon nitride, is a purely organic semiconductor material composed of the earth-abundant light elements carbon and nitrogen.^{12,13} One of its morphology-wise modified analogues, called

mesoporous graphitic carbon nitride (mpg-CN), is especially attractive as a heterogeneous catalyst due to its larger surface area.^{14,15} This polymeric material possesses suitable valence band maxima (VBM) and conduction band minima (CBM), spanning a band gap of approximately 2.7 eV upon visible light photoexcitation. Although mpg-CN is yet to be commercialized, the cost of its synthesis falls within the range of a few euros/kg due to its inexpensive synthetic precursors (e.g., urea and melamine) and easy synthetic procedures (see the [Supporting Information](#)).¹⁶ Owing to its outstanding thermal, chemical, and photostability, mpg-CN has found applications in various fields such as hydrogen production by overall water splitting,¹² carbon dioxide reduction^{17,18} as well as in several synthetic transformations.¹⁵ Surprisingly, mpg-CN has rarely been used as a photocatalyst for direct C(sp³)–H functionalization by hydrogen atom transfer (HAT) chemistry.^{19,20} The synergistic combination of homogeneous photocatalysis, HAT, and transition-metal catalysis has provided several methods for selective C–H bond functionalization,^{21–23}

Received: December 29, 2020

Revised: January 6, 2021

Published: January 19, 2021



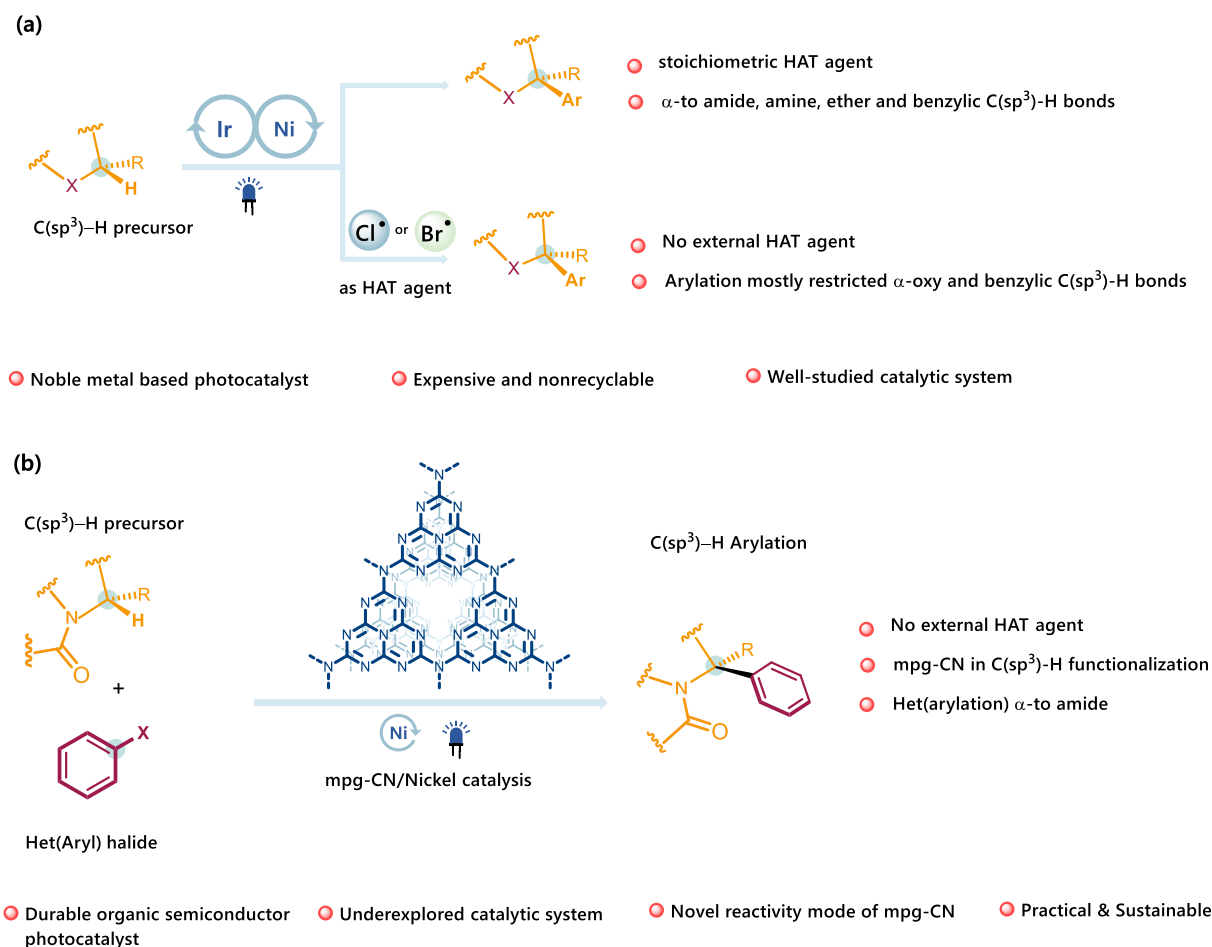


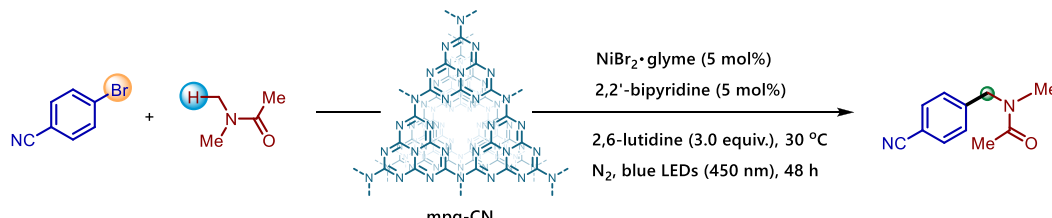
Figure 1. Schematic representation of different photocatalytic systems for C(sp³)-H arylation. (a) Homogeneous photocatalytic system for C(sp³)-H arylation with aryl halides. (b) The present study: mpg-CN photocatalytic C(sp³)-H arylation of amides.

most of which remain restricted to the use of either (i) activated Michael acceptors (electron-deficient olefins)^{24–26} or (ii) stoichiometric amounts of HAT agents.²⁷ Recently, halogen radicals are shown to act as effective HAT agents for C–H functionalizations (Figure 1a).²⁸ Inspired by the pioneering works of Doyle,^{28b} Murakami,^{28f} and Wu,²¹ we anticipated that the catalytically formed halogen radicals on the mpg-CN surface might participate in a HAT event for the generation of carbon radicals, which in combination with transition metal catalysis would enable arylation of C(sp³)-H bonds with aryl halides in a redox-neutral fashion.²⁹

Herein, we describe the mpg-CN photocatalytic arylation of C(sp³)-H bonds in combination with nickel catalysis,³⁰ as a robust, practical, and tolerant protocol even suitable for late-stage functionalization of bioactive molecules (Figure 1b). The reaction is selective for C–H activations α to amide groups. Mechanistic investigations and kinetic studies suggest energy transfer (EnT) from the organic semiconductor to the nickel metal center as a new reaction mode distinguishing this reaction from typical semiconductor single electron transfer (SET) process. The synergistic use of HAT and EnT³¹ as mediated via a heterogeneous semiconductor photocatalyst is a concept expected to greatly expand the boundaries of synthetic photocatalysis.

We focused our investigation on the activation of the C(sp³)-H bond adjacent to the nitrogen atom of amides due to the importance of this functional group. Particularly, benzyl

amines with *N*-electron-withdrawing groups are a prominent substructure in drugs, such as compounds for the treatment of plaque psoriasis, seizures, and diabetes.³² In a typical synthesis, they are prepared through alkylation of amides with benzyl halides, but the chemical diversity of commercially available benzyl halides is limited. In contrast, the direct C–H arylation α to amide *N*-atom constitutes a potentially better approach considering the available large number of aryl halides in chemical feedstocks, drug molecules, and natural products. As a model system, 4-bromobenzonitrile was employed toward the C(sp³)-H bond arylation of *N,N*-dimethyl acetamide (DMA) as both C–H precursor and solvent. Table 1 summarizes the optimization of the reaction parameters and control experiments (see the Supporting Information for additional data). After systematic evaluation of various nickel(II) salts, ligands, and bases, we found that a mixture consisting of NiBr₂·glyme, 2,2′-bipyridine, 2,6-lutidine, and mpg-CN under blue light-emitting diode (LED; 450 ± 15 nm) irradiation at ambient temperature furnished the best result for our desired transformation, obtaining 1a in an 85% isolated yield after 48 h (Table 1, entry 1). The dehalogenation of the starting material (i.e., benzonitrile) was the only detectable side product of the reaction. The reaction only required simple mixing of all of the components in a vial followed by photoillumination. Control experiments, which are either performed without mpg-CN, [Ni] catalyst, light, or ligand, revealed the necessity of each component for this novel C–C

Table 1. Selected Optimization and Control Experiments for mpg-CN Photocatalyzed C(sp³)–H Bond Arylation


Entry	Deviation from standard conditions ^a	Yield (%) ^b
1.	None	90(85) ^c
2.	no mpg-CN	ND
3.	no NiBr ₂ ·glyme	ND
4.	no light	ND
5.	no ligand	<5
6.	no 2,6-lutidine	11
7.	no [Ni] catalyst & recovered mpg-CN	ND
8.	dtbbpy instead of bpy	52
9.	K ₃ PO ₄ instead of 2,6-lutidine	13
10.	no degassing and under N ₂	74
11.	under air	59
12.	NiBr ₂ ·3H ₂ O instead of NiBr ₂ ·glyme	72

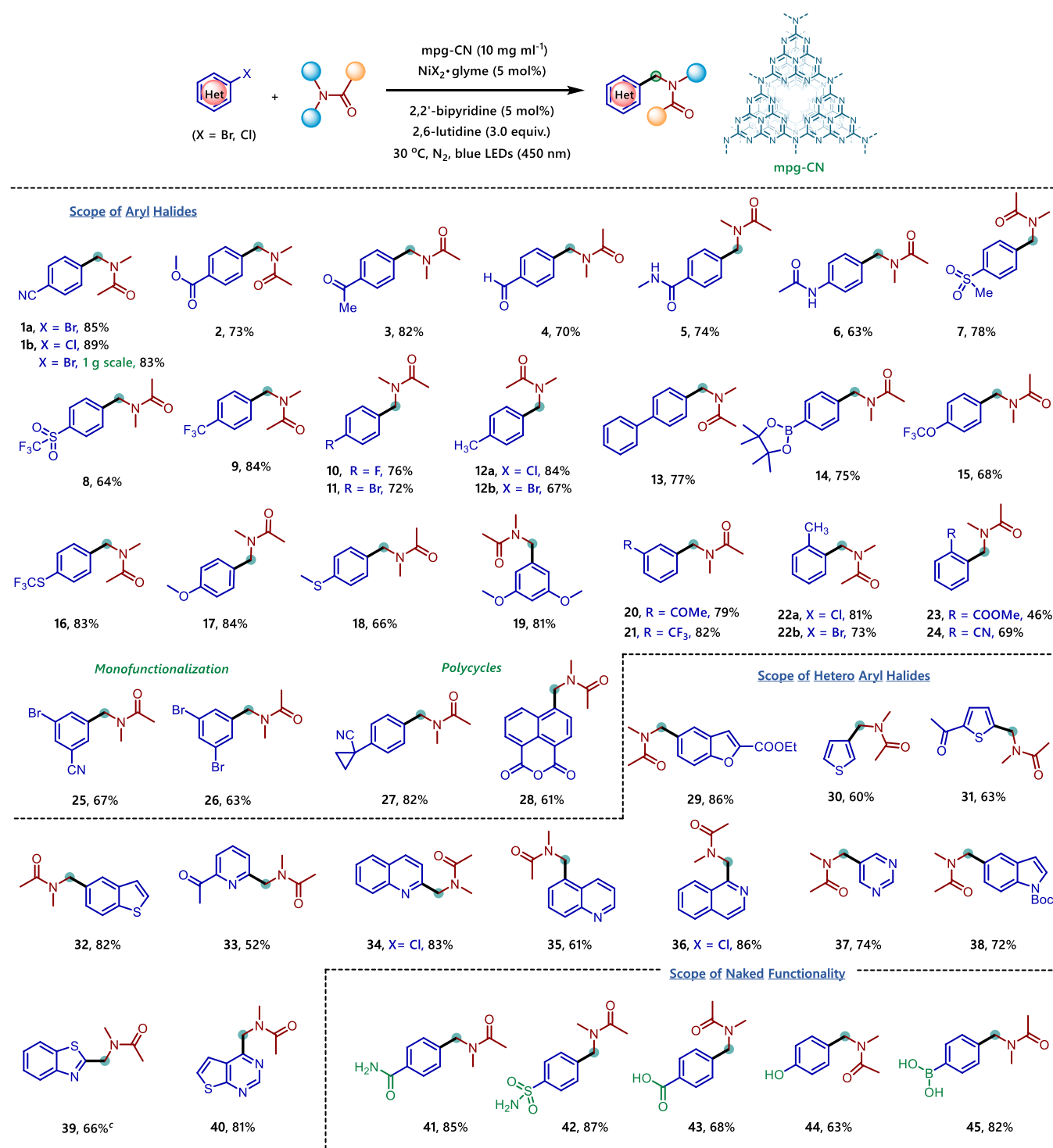
^aReaction conditions: 4-bromobenzonitrile (36.4 mg, 0.2 mmol), mpg-CN (10 mg), NiBr₂·glyme (3.2 mg, 5.0 mol %), 2,2'-bipyridine (1.6 mg, 5.0 mol %), and 2,6-lutidine (70 μL, 3.0 equiv) in 1 mL DMA under blue light irradiation (450 ± 15 nm) at 30 °C for 48 h. ^bYields were determined by gas chromatography-flame ionization detector (GC-FID) using 1,4-dimethoxybenzene as an internal standard. ^cYield of the isolated product. ND, not detected.

bond-forming reaction (entries 2–5). Curiously, even in the absence of 2,6-lutidine, the reaction proceeded to some extent, possibly due to the basic nature of the bipyridine ligand (entry 6). The employment of recycled mpg-CN, without the renewed addition of [Ni] catalyst, failed to afford the reaction product, corroborating the absence of active nickel catalyst remaining on the surface of the heterogeneous photocatalyst (entry 7). Unsubstituted bipyridine (bpy) served as the optimal ligand system, which is cheaper than dtbbpy(4,4'-di-*tert*-butyl-2,2'-bipyridine), the most commonly employed ligand in metallaphotoredox chemistry (entry 8). The choice of base is a crucial parameter since most of the commonly employed inorganic or organic bases were ineffective in the reaction (entry 9 and Table S3). Ultimately, the use of 2,6-lutidine as a base proved to be optimal for this transformation. Comparable yields were also obtained without degassed solvents or under air (entries 10 and 11) or with inexpensive NiBr₂·3H₂O as nickel source (entry 12), thus showcasing the robustness of the mpg-CN photocatalytic C(sp³)–H bond arylation method.

With the optimized reaction conditions in hand, we next explored the scope of the mpg-CN/nickel-catalyzed arylation process. Initially, we examined the generality of aryl halides as partners. As evident from the examples listed in Table 2, a diverse multitude of aryl halides bearing either electron-donating or electron-withdrawing substituents underwent C(sp³)–H arylation with DMA. Notably, mpg-CN photocatalytic C–H arylation displayed an excellent chemoselectivity profile. For example, nitrile (1a), ester (2), ketone (3), aldehyde (4), amides (5, 6), sulfone (7), and trifluoromethyl sulfone (8) were tolerated. In addition, aryl boronic acid pinacol ester (14) and electrophilic sites that are

sensitive to Ni-catalyzed cross-coupling reactions such as aryl halides (10, 11) were also accommodated, thus providing handles for further functionalization. Aryl bromides, containing –CF₃ (9), –OCF₃ (15), or –SCF₃ (16) groups, which are privileged functionalities in pharmaceuticals and agrochemicals, underwent arylation in good to excellent yields (68–84%). Moderately electron-donating (12b) or electronically neutral (13) groups on the aryl moiety were well tolerated despite the propensity for homolytic C–H bond cleavage at the benzylic position of 12b. In terms of the arene partner, the efficacy of the reaction was hardly impacted by either (i) a change in electronic properties from *meta*-substitution (20, 21) or (ii) sterically encumbrance from *ortho*-substitution (22b, 23, 24). The reaction was very good, compatible with highly electron-rich aryl bromides among which the sulfide- (18) or dimethoxy (19)-containing moieties are particularly worth mentioning as they are generally considered to be labile toward oxidation by molecular photocatalysts. Gratifyingly, our method could be extended to aryl chlorides and 1b, 12a, and 22a were obtained in excellent yields (81–89%). Aryl moieties having more than one reactive site (25, 26) are selectively monofunctionalized, thus allowing room for additional functionalization. The mpg-CN photochemical protocol was even effectively employed to polycyclic aryl bromides (27, 28) in spite of their tendency toward ring-opening reaction in the presence of a nickel catalyst.

Pleasingly, the developed conditions easily translated on a gram scale in batch-mode processing without noticeable erosion in yield (1a, 83%). Elsewhere, continuous flow chemistry is widely appreciated as an enabling technology for the scale-up of photochemical processes.³³ Scalability was evaluated³⁴ in two commercially available suspension/slurry-

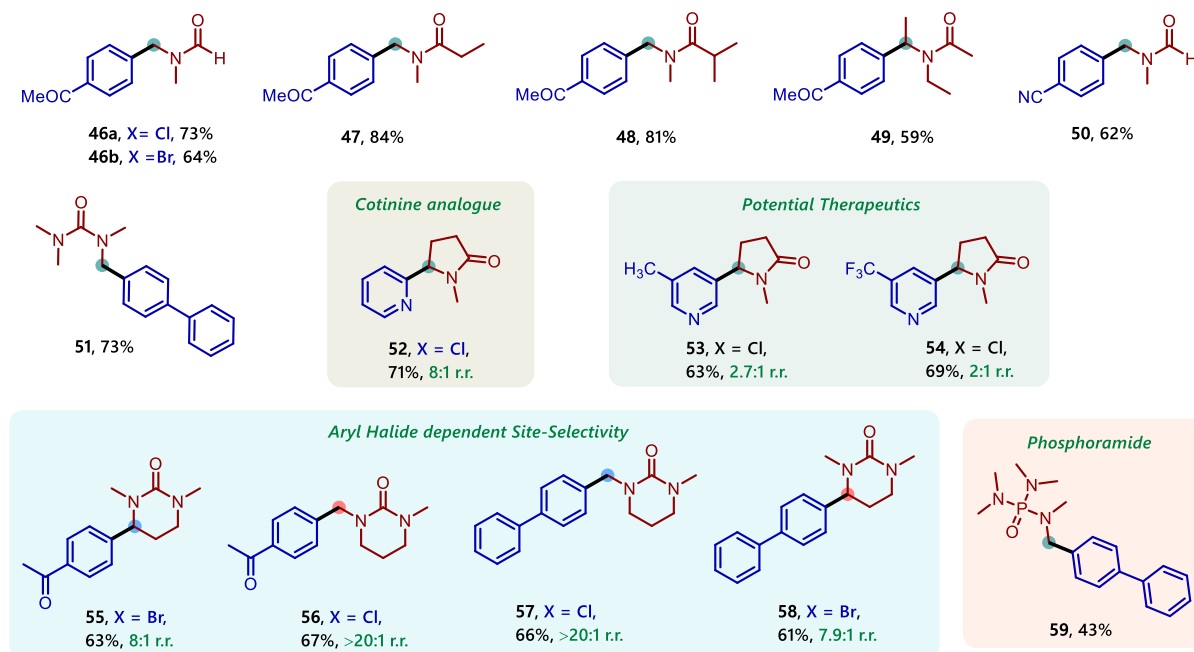
Table 2. Scope of (Hetero)aryl Halides^{a,b,c}

^aReaction conditions: as Table 1 (entry 1). ^bYields of the isolated products. ^c1.0 equiv tetrabutylammonium chloride was used as an additive. Unless otherwise stated, products derive from their (hetero)aryl bromide precursors.

handling continuous flow reactors (10–15 mL reactor sizes), one tubular reactor and one that used state-of-the-art oscillatory flow and pulsation technology together with hi-power LED modules (24–45 W radiant power). Surprisingly, preliminary results found conversion and productivity (mg/h) inferior to that obtained on gram scale in a batch reactor (100 mL reactor size). While further studies are necessary to understand and remedy this surprising observation, we

postulate that the mismatched time domains of a faster-flowing liquid phase and slower-flowing solid particles in a continuously flowing stream are counterproductive for adsorption of reactive species to the mpg-CN surface in the context of the photocatalytic chemistry herein (see the Supporting Information for a detailed investigation).

Next, the amenability toward heteroaryl halides was assessed. Notably, our protocol displayed an exceptional level

Table 3. Scope of C(sp³)–H Precursors^{a,b}

^aYields of the isolated products. ^bSee the Supporting Information for (hetero)aryl halide precursors. r.r. = regioisomeric ratio.

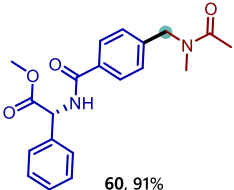
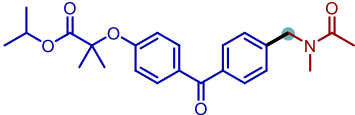
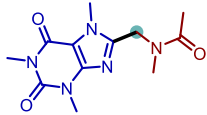
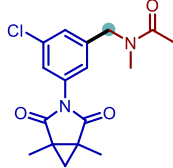
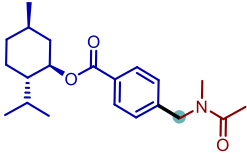
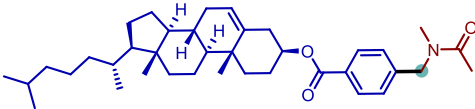
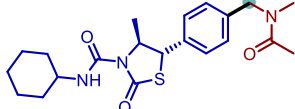
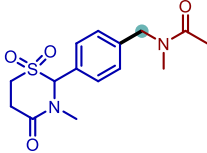
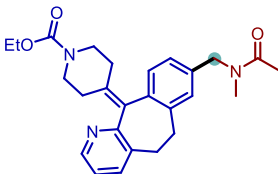
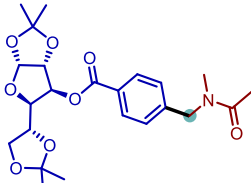
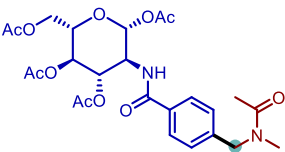
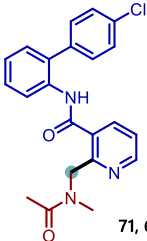
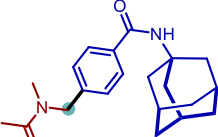
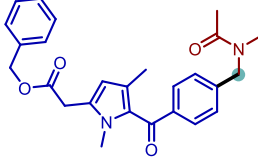
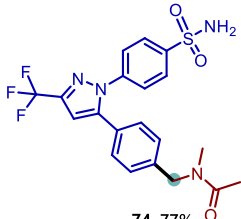
of tolerance toward a broad range of heteroaryl bromides as well as chlorides (Table 2). A wide variety of electron-poor nitrogen-containing heterocycles such as pyridine (33), quinolines (34, 35), isoquinoline (36), pyrimidine (37), indole (38), benzothiazole (39), and thieno[2,3-*d*]pyrimidine (40) could all be functionalized. We note that such nitrogen-containing heterocycles bearing an amide functionality are typical scaffolds in many active pharmaceutical ingredients. Moreover, electron-rich heterocycles such as benzofuran (29), thiophene (30, 31), and benzothiophene (32) were also well tolerated. The robustness of mpg-CN photocatalysis compared to that of metallaphotoredox reactions of iridium polypyridyl complexes is a potential advantage. The iridium complexes can lead to lower product yields of electron-rich heterocycles due to competing SET processes.²⁸

We then tested the compatibility of our mpg-CN photocatalytic arylation method with unprotected polar functional groups, an important criterion for assessing a method's robustness and applicability toward drug discovery and the synthesis of bioactive molecules. Strikingly, aryl bromides containing unprotected amide, sulfonamide, carboxylic acid, phenol, or boronic acid functionalities all reacted smoothly and afforded the desired products (41–45) in excellent yields (Table 2). For instance, the free –OH group in 44 remains untouched even though phenolic compounds are typically sensitive toward oxidation under photochemical conditions. The presence of boronic acid in 45 demonstrates (i) the orthogonality of our protocol compared to that of classical metal-catalyzed cross-coupling reactions and (ii) our protocol's tolerance of a valuable handle for further synthetic transformations.

Encouraged by the aforementioned results, we expanded the mpg-CN semiconductor photocatalytic arylation method to C–H precursors other than DMA.³⁵ Gratifyingly, this was possible, and a variety of acyclic and cyclic amides could be employed as C(sp³)–H bond functional handles with similar

results to DMA. *N,N*-Dimethyl-formamide, -propionamide, and -isobutyramide all furnished their corresponding arylated products (46–48, 50) in good to excellent yields (62–84%). Even a more sterically encumbered secondary C(sp³)–H position of *N,N*-diethylacetamide (49) could be functionalized, albeit in slightly lower yields. Here, it is worth mentioning that C–H arylation could also be performed in acetonitrile as solvent using 10 equivalents of amide C–H precursor and catalytic amounts of tetrabutylammonium chloride as an additive.³⁶ We were quite surprised to find that C(sp³)–H arylation of *N*-methyl-2-pyrrolidone (NMP) with 2-chloropyridine rapidly afforded the corresponding cotinine analogue (52) in very good yield and excellent regioselectivity. Although 3-chloropyridine derivatives provided diminished regioselectivity, cotinine 53, the methyl analogue of a potential therapeutic agent against Alzheimer's disease,³⁷ is not easily accessible by conventional synthetic methods and its –CF₃ derivative 54 has not been described. We observed high regioselectivity for methyl and methylene C–H bonds by choosing appropriate aryl halides. A cyclic urea derivative reacted preferentially at its *N*-CH₂ position in the presence of aryl bromides (55, 58), whereas the same derivative reacted exclusively at its *N*-CH₃ position in the presence of aryl chlorides (56, 57). This preference for activation of the least-substituted C–H bond by Cl radicals and activation of the most-substituted C–H bond by Br radicals reflects a previous report concerning C(sp³)–H functionalization of hydrocarbons.²⁴ While such exclusive selectivity for *N*-CH₃ functionalization in the presence of *N*-CH₂ positions has been reported for alkylamines,³⁸ this is not the case for alkylamides. Interestingly, most of the compounds shown in Table 3 have not been prepared before, illustrating the capability of our method to branch into new chemical space. For example, the successful arylation of hexamethylphosphoramide (59) as a C–H precursor provided rapid access to benzylamine derivatives with potential physiological activity.

Table 4. Application of the mpg-CN Photocatalytic C(sp³)–H Arylation Method to Bioactive Molecules^{a,b}

 <p>60, 91% From (R)-(-)-2-Phenylglycine</p>	 <p>61, 83% From Fenofibrate: lipid lowering</p>	 <p>62, 72% From Caffeine</p>	 <p>63, 67% From Procymidone: pesticide, androgen receptor antagonist</p>
 <p>64, 79% From (-)-Menthol</p>	 <p>65, 71% From Cholesterol</p>	 <p>66, 68% From Hexythiazox acaricide</p>	
 <p>67, 76% From Chlormezanone: anxiolytic</p>	 <p>68, 63% From Loratadine: antihistamine</p>	 <p>69, 74% From D-Glucose diacetonide</p>	 <p>70, 74% From Glucosamine</p>
 <p>71, 61% From Boscalid: fungicide</p>	 <p>72, 64% From Ladasten (bromantane) analogue: immunostimulant, Parkinson's disease</p>	 <p>73, 58% From Zomepirac NSAID-antipyretic</p>	 <p>74, 77% From Br-Celecoxib: COX-2 inhibitor, osteoarthritis, ankylosing spondylitis</p>

^aYields of the isolated products. ^bSee the Supporting Information for (hetero)aryl halide precursors.

Finally, we demonstrated the application of our mpg-CN photocatalytic C(sp³)–H arylation method to the late-stage functionalization of bioactive molecules, including pharmaceuticals, hormones, and agrochemicals (pesticide, fungicide) as aryl coupling components, and were delighted to observe the desired products (**60**–**74**) in good to excellent yields (Table 4). Our protocol therefore enlarges the palette of opportunities for modern applications in drug discovery and agrochemicals.

Apart from innate chemical and photostability, one of the prime advantages of mpg-CN is its heterogeneous nature that allows straightforward recovery of the catalyst from the reaction mixture and the recovered catalyst can be reused multiple times preserving its photocatalytic reactivity. As demonstrated in Figure 2a, mpg-CN photocatalyst can at least be recycled five times without appreciable loss in the product yield. The recovered material was characterized by a series of techniques used for the characterization of fresh mpg-CN (see the Supporting Information for details) such as Fourier transform infrared spectroscopy (FT-IR), powder X-ray diffraction (PXRD), energy-dispersive X-ray analysis (EDX), inductively coupled plasma optical emission spectrometry (ICP-OES), transmission electron microscopy (TEM),

etc. The position and intensity of all peaks in FT-IR spectrum and PXRD pattern revealed that the bulk chemical structure of the recovered photocatalyst was unchanged (Figures S14 and 2b), while EDX and XPS elemental analysis showed enhanced oxygen content on the surface of the recovered photocatalyst (Tables S7 and S8). Additionally, ICP-OES experiments identified that 0.07 ± 0.013 wt. % Ni contained in the recovered mpg-CN (Table S9). Interestingly, Ni 2p XPS did not show any distinct signal of nickel (Figure S24). Considering that XPS is a surface-sensitive technique, such an apparently anomalous result confirmed that nickel in the sample is mainly located in the bulk of the material. Similarly, no signal was observed in Br 3d XPS, which could potentially be related to using NiBr₂ as a metal precursor (Figure S25). High-resolution (HR)-TEM images of the recovered mpg-CN (i) indicated that its mesoporous structure was retained and (ii) revealed the presence of dark spots with a diameter of 2–6 nm. These could be attributed to the formation of Ni(0) nanoparticles (Figure 2c). Indeed, deposition of Ni black, albeit significantly larger amounts (1.4–12.6 wt. %) compared to ~0.07 wt. % in this work, has been previously reported.^{39,40} N 1s XPS indicated the dicoordinated nitrogen of C=N–C moieties in a tri-s-triazine unit as observed in the

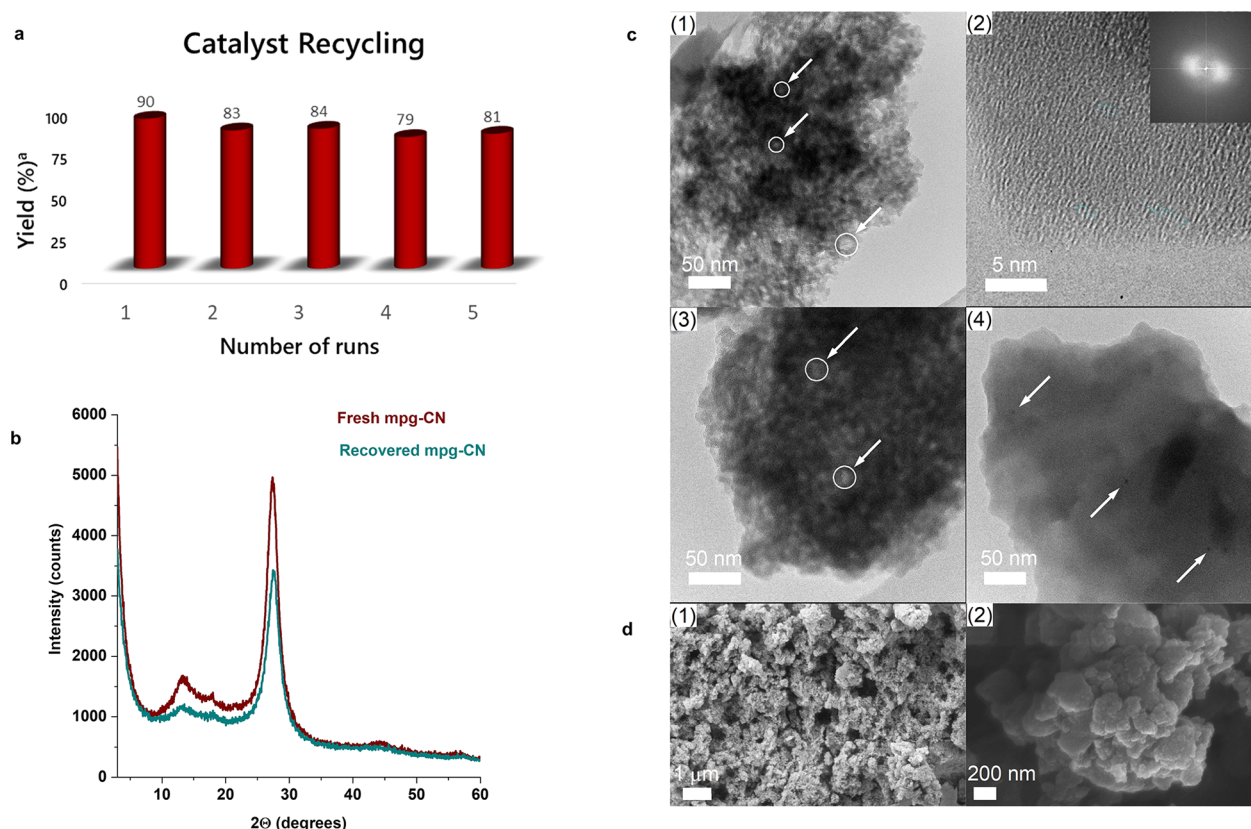
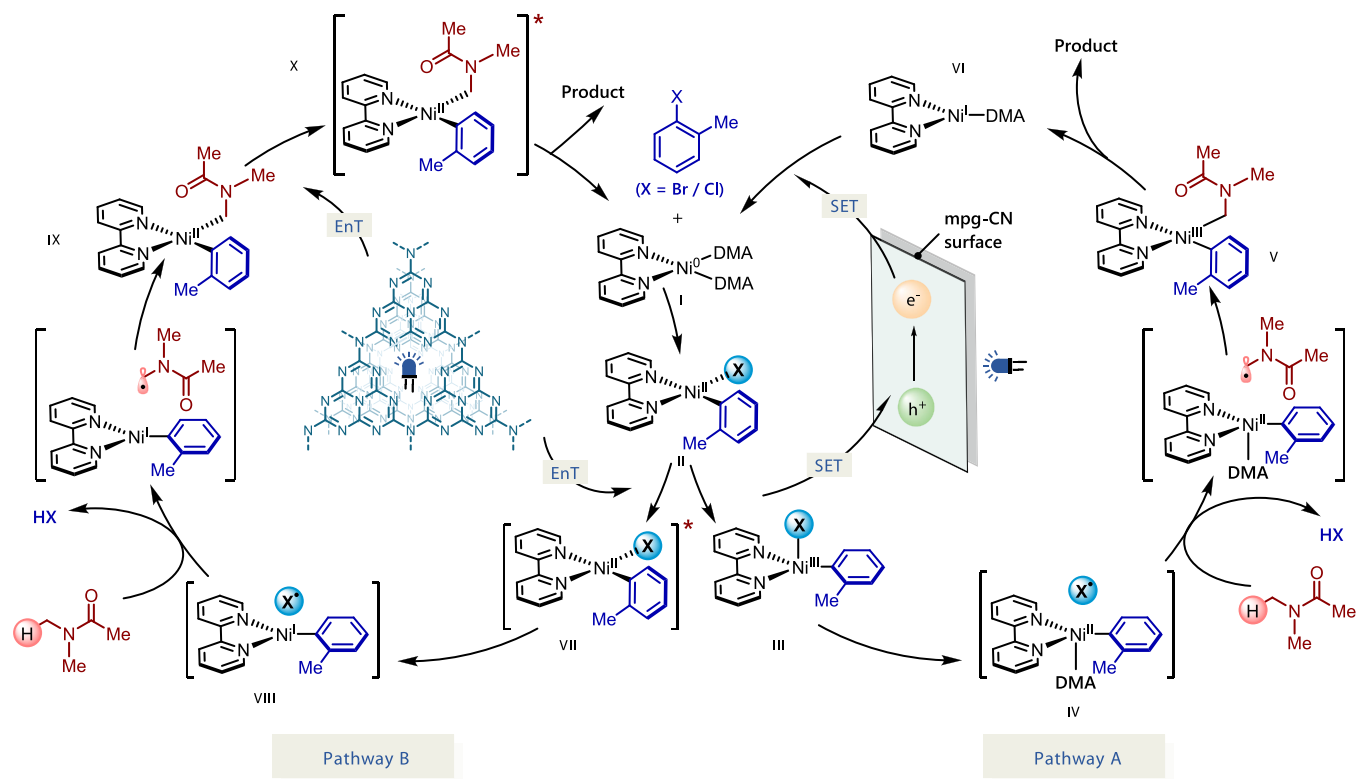


Figure 2. Characterization of fresh and recovered mpg-CN. (a) Evaluation of catalytic recycling. (b) PXRD pattern of fresh and recovered mpg-CN. (c) TEM images of the photocatalyst: (1) fresh mpg-CN, overview image, circles mark mesopores; (2) HR-TEM image of fresh mpg-CN with the corresponding fast Fourier transform (FFT) as the inset; (3) recovered mpg-CN, overview image, circles mark mesopores; and (4) recovered mpg-CN, arrows indicate Ni(0) nanoparticles. (d) SEM images of fresh mpg-CN (1) and recovered (2).

Scheme 1. Plausible Mechanistic Pathways for mpg-CN/Nickel Photocatalytic C(sp³)-H Arylation



fresh catalyst (Figure S16). The abundance of nitrogen atoms renders the material as an effective polydentate ligand to coordinate nickel atoms. Coordination with the covalent carbon nitride mpg-CN gives rise to a 16-electron Ni(II) chelate complex compared to that of a more reactive 14-electron Ni(II)-amide complex in the case of ionic carbon nitrides (Figure S26). These observations indicate that the problem of nickel black formation in dual Ni/photoredox catalysis (in addition to adjusting the rates of oxidative addition and reductive elimination by tuning the energy of incident light and the concentration of reagents)³⁹ could also be eliminated by using a robust carbon nitride photocatalyst that stabilizes the low valent nickel species without altering the overall reaction rates. The recovered mpg-CN showed a slight shift of the absorption onset in the DRUV-vis spectrum and an expansion of the optical band gap by ~ 0.05 eV (Figure S20). In steady-state photoluminescence (PL), surface modification of mpg-CN is observed as a blue shift in fluorescence by ~ 0.1 eV (Figure S21).

The morphology of the recovered mpg-CN particles adopted a more rounded shape compared to that of a rougher surface of freshly prepared mpg-CN (Figure 2d). Taken together, the postcharacterization data of the recovered mpg-CN clearly shows robustness, stability, and durability of this heterogeneous organic semiconductor as a photocatalyst.

The aforementioned results provide evidence for catalytic generation of HAT agent on the mpg-CN semiconductor surface, which operates in synergy with nickel catalysis to enable C(sp³)-H bond functionalization. However, the photoactivity of mpg-CN/nickel dual catalytic system for C-H bond cleavage at a molecular level remains to be elucidated. Based on prior mechanistic investigations of dual Ni/photocatalyzed cross-coupling reactions in homogeneous systems,⁴¹ we postulate two plausible mechanistic scenarios as depicted in Scheme 1. Initially, the Ni(0) complex I undergoes oxidative addition with an aryl halide delivering Ni(II) oxidative addition complex II. Concurrently, light absorption by the mpg-CN semiconductor photocatalyst triggers the charge separation producing two-dimensional surface redox centers as electron-hole pairs. In pathway A, SET oxidation of complex II by the photogenerated hole (VBM located at +1.2 V vs SCE, $E_{1/2}$ (Ni^{II}/Ni^{III}) = +0.85 V vs SCE) affords species III, which may undergo Ni(III)-X homolysis to give a halogen radical and Ni(II) species IV.²⁸ The resulting halogen radical can rapidly abstract a hydrogen atom from DMA (H-Br BDE ~ 88 kcal/mol, H-Cl BDE ~ 102 kcal/mol, α -amino C-H BDE ~ 89 –94 kcal/mol),²⁷ which immediately recombines with species IV to form V. Subsequent reductive elimination of V results in the desired product and Ni(I) species VI. Finally, reduction of VI by the electron located on the semiconductor surface (CBM located at -1.5 V vs SCE, $E_{1/2}$ (Ni^I/Ni⁰) = -1.42 V vs SCE)⁴¹ regenerates Ni(0) and completes the catalytic cycle. In pathway B, mpg-CN serves as a light-absorbing antenna undergoing an energy-transfer process (EnT) (singlet-triplet band gap ca. 0.39 eV)⁴² to produce electronically excited Ni(II) species VII. Homolysis of the Ni(II)-X bond and HAT followed by a rebound of the resulting carbon-centered radical with VIII generates Ni(II) species IX. Reductive elimination from the electronically excited species X, promoted by EnT with mpg-CN, provides the final product and regenerates Ni(0) species, thus completing the catalytic cycle.

Control experiments with a catalytic amount of preformed [(bpy)Ni^{II}(*o*-tolyl)Br] complex II in our standard reaction conditions (Table 5) show that both complex II and mpg-CN

Table 5. Catalytic Experiments with Preformed [(bpy)Ni^{II}(*o*-tolyl)Br] Complex II^{a,b}

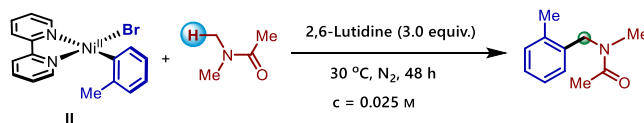


entry	deviation from the above condition	yield (%)
1.	none	5
2.	with mpg-CN (10 mg/mL)	56

^aWith 5 mol % II. ^bYields were determined by GC-FID using 1,4-dimethoxybenzene as an internal standard.

are required in the productive reaction pathway. A major distinction between these two pathways, as shown in Scheme 1, is that EnT process involves the excited state of Ni(II) species, which should be directly accessible via visible light excitation in the absence of photocatalyst (Figure S27). Indeed, a stoichiometric experiment with [(bpy)Ni^{II}(*o*-tolyl)Br] complex II via direct photoexcitation at 450 nm (i.e., without mpg-CN) revealed the formation of the desired product in appreciable yield (Table 6). An additional control

Table 6. Stoichiometric Experiments with Preformed [(bpy)Ni^{II}(*o*-tolyl)Br] Complex II^{a,b}



entry	light source	yield
1.	340 nm	17%
2.	450 nm	20%
3.	dark	ND

^aSee the Supporting Information for details. ^bYields were determined by GC-FID using 1,4-dimethoxybenzene as an internal standard.

experiment performed under identical conditions in the absence of light failed to produce any detectable product. These experiments are indicative toward pathway B where the formation of an electronically excited Ni(II) complex is a prerequisite for bond formation.

The reaction kinetics were monitored at different concentrations of the nickel complex as well as aryl bromide. In all cases, we observed a zero-order kinetic profile (Figure 3) at room temperature (Table S14), which is a typical behavior of heterogeneous catalytic reactions in which active sites are saturated by adsorbed reactant molecules. Similar observations have been reported previously for carbon nitride/nickel dual photocatalysis.⁴³ Interestingly, increasing the [Ni] loading by three times increased the relative amount of debrominated product and halved the reaction rate (Figure 3a vs b). This could be ascribed to saturating the mpg-CN active sites while having more [Ni] complexes in solution. As a result, the [Ni] complex, which is involved in the rate-determining step, has to compete with other off-cycle or non-rate-determining on-cycle [Ni] complexes for mpg-CN active sites leading to the overall

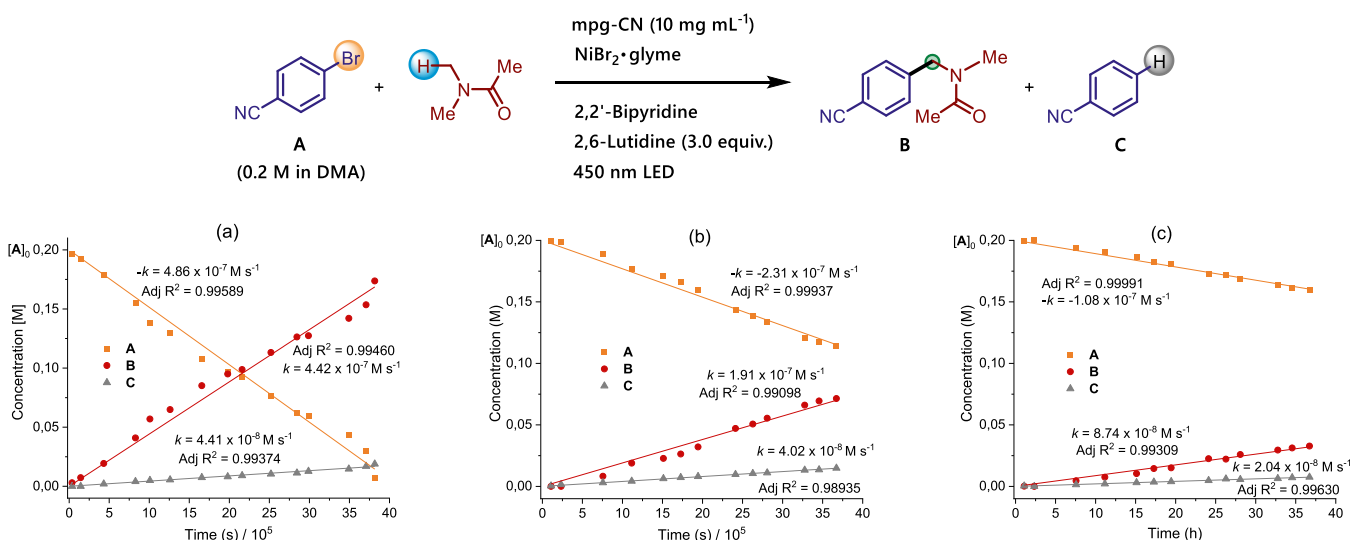


Figure 3. Reaction kinetic profile for Ni/mpg-CN photocatalytic arylation. Reaction conditions: 4-bromobenzonitrile (A) (0.2 mmol), mpg-CN (10 mg/mL), 2,6-lutidine (3.0 equiv), and DMA (0.2 M with respect to A) under 450 nm blue light irradiation at 25 °C: (a) with 5 mol % NiBr₂·glyme and 5 mol % 2,2'-bipyridine, (b) with 15 mol % NiBr₂·glyme and 2,2'-bipyridine, and (c) with 0.6 M of (A) in DMA at 25 °C.

decline in rate. Likewise, increasing the concentration of 4-bromobenzonitrile further decreased the reaction rate (Figure 3a vs c). Such rate dependence on nickel and haloarene concentration indicates that the rate-determining step occurs as a result of adsorption of species at the mpg-CN surface.⁴³ Given that EnT processes are only efficient over short distances, effective adsorption may be more critical to an EnT mechanism than a SET mechanism, which can occur over longer distances assisted by solvent molecules.⁴⁴ Nevertheless, we cannot rule out the possibility of a disproportionation reaction between photoexcited Ni(II)* and ground-state Ni(II) to give Ni(I) and Ni(III) species followed by reductive elimination to afford the product. However, the low concentration, as well as the short lifetime of the Ni(II)* complex (ca. $\tau = 2.53 \text{ ns}$ for [(bpy)Ni^{II}(*o*-tolyl)Br]), makes this mechanism very unlikely to be a major contributing pathway.⁴⁴

We have demonstrated the so far unrecognized potential of mesoporous graphitic carbon nitride (mpg-CN) in direct (hetero)arylations of C(sp³)-H bonds via a synergistic combination with nickel catalysis. Catalytically generated halogen radicals act as hydrogen atom transfer agents for the functionalization of C(sp³)-H bonds while tolerating a large number of functional groups. The protocol, based on a durable organic semiconductor mpg-CN photocatalyst and a simple nickel catalyst, provides a powerful alternative to conventional homogeneous photoredox catalysts. From a sustainable chemistry perspective, our protocol offers a distinct advantage over others. Namely, its heterogeneous nature means that mpg-CN is readily recovered from the reaction media by simple centrifugation and can be reused multiple times without appreciable loss in activity. Gram-scale reactions are possible in batch, where batch-processing surprisingly provided a more viable option for scale-up than continuous flow using dedicated slurry-handling oscillatory flow reactors. Mechanistic investigations provide evidence of an energy-transfer-driven pathway generating an electronically excited nickel complex as a reactive intermediate. Finally, the potentiality of mpg-CN as an attractive visible light-absorbing organic semiconductor photocatalyst has been demonstrated by performing late-stage

functionalization on complex molecules. Considering the use of bioactive (hetero)aromatic halides as potential coupling partners, this cost-effective technology may find applications in modern drug discovery. Finally, we believe that the distinct reactivity mode of mpg-CN described herein may lead to novel designs in EnT catalysis.

■ ASSOCIATED CONTENT

Supporting Information

The Supporting Information is available free of charge at <https://pubs.acs.org/doi/10.1021/acscatal.0c05694>.

Experimental details, characterization data for the products, and supporting crystallographic data (PDF)

■ AUTHOR INFORMATION

Corresponding Author

Burkhard König – Fakultät für Chemie und Pharmazie, Universität Regensburg, 93040 Regensburg, Germany; orcid.org/0000-0002-6131-4850; Email: burkhard.koenig@ur.de

Authors

Saikat Das – Fakultät für Chemie und Pharmazie, Universität Regensburg, 93040 Regensburg, Germany; orcid.org/0000-0002-8698-9205
 Kathiravan Murugesan – Fakultät für Chemie und Pharmazie, Universität Regensburg, 93040 Regensburg, Germany
 Gonzalo J. Villegas Rodríguez – Fakultät für Chemie und Pharmazie, Universität Regensburg, 93040 Regensburg, Germany
 Jaspreet Kaur – Fakultät für Chemie und Pharmazie, Universität Regensburg, 93040 Regensburg, Germany
 Joshua P. Barham – Fakultät für Chemie und Pharmazie, Universität Regensburg, 93040 Regensburg, Germany
 Aleksandr Savateev – Department of Colloid Chemistry, Max-Planck Institute of Colloids and Interfaces, 14424 Potsdam, Germany; orcid.org/0000-0002-5760-6033

Markus Antonietti – Department of Colloid Chemistry, Max-Planck Institute of Colloids and Interfaces, 14424 Potsdam, Germany; orcid.org/0000-0002-8395-7558

Complete contact information is available at:
<https://pubs.acs.org/10.1021/acscatal.0c05694>

Notes

The authors declare no competing financial interest.

ACKNOWLEDGMENTS

The German Science Foundation (DFG, KO 1537/18-1) supported this work. This project has received funding from the European Research Council (ERC) under the European Union's Horizon 2020 Research and Innovation Programme (grant agreement No. 741623). We thank Dr. Rudolf Vasold for GC-MS measurements and Regina Hoheisel for cyclic voltammetry measurements. We also thank Jiamei Liu at the Instrument Analysis Center of Xi'an Jiaotong University for her assistance with XPS analysis and Bolortuya Badamdorj for acquiring TEM images. We thank Dr. Hannes Gemoets for his helpful discussions and CreaFlow for providing an oscillatory flow reactor (HANU reactor) and Peschl Ultraviolet GmbH for providing an appropriate hi-power LED module.

REFERENCES

- (1) (a) Stephenson, C.; Yoon, T. P. Enabling Chemical Synthesis with Visible Light. *Acc. Chem. Res.* **2016**, *49*, 2059–2060. (b) Marz, L.; Pagire, S. K.; Reiser, O.; König, B. Visible-Light Photocatalysis: Does It Make a Difference in Organic Synthesis? *Angew. Chem., Int. Ed.* **2018**, *57*, 10034–10072. (c) Prier, C. K.; Rankic, D. A.; MacMillan, D. W. C. Visible Light Photoredox Catalysis with Transition Metal Complexes: Applications in Organic Synthesis. *Chem. Rev.* **2013**, *113*, 5322–5363.
- (2) (a) Schultz, D. M.; Yoon, T. P. Solar Synthesis: Prospects in Visible Light Photocatalysis. *Science* **2014**, *343*, No. 1239176. (b) Yoon, T. P.; Ischay, M. A.; Du, J. Visible light photocatalysis as a greener approach to photochemical synthesis. *Nat. Chem.* **2010**, *2*, 527–532. (c) Margrey, K. A.; Czaplyski, W. L.; Nicewicz, D. A.; Alexanian, E. J. A General Strategy for Aliphatic C–H Functionalization Enabled by Organic Photoredox Catalysis. *J. Am. Chem. Soc.* **2018**, *140*, 4213–4217.
- (3) Cernak, T.; Dykstra, K. D.; Tyagarajan, S.; Vachal, P.; Krska, S. W. The medicinal chemist's toolbox for late stage functionalization of drug-like molecules. *Chem. Soc. Rev.* **2016**, *45*, 546–576.
- (4) (a) Lyons, T. W.; Sanford, M. S. Palladium-Catalyzed Ligand-Directed C–H Functionalization Reactions. *Chem. Rev.* **2010**, *110*, 1147–1169. (b) He, J.; Wasa, M.; Chan, K. S. L.; Shao, Q.; Yu, J. Q. Palladium-Catalyzed Transformations of Alkyl C–H Bonds. *Chem. Rev.* **2017**, *117*, 8754–8786. (c) Liao, K.; Pickel, T. C.; Boyarskikh, V.; Bacsa, J.; Musaev, D. G.; Davies, H. M. L. Site-selective and stereoselective functionalization of non-activated tertiary C–H bonds. *Nature* **2017**, *551*, 609–613.
- (5) Shaw, M. H.; Twilton, J.; MacMillan, D. W. C. Photoredox Catalysis in Organic Chemistry. *J. Org. Chem.* **2016**, *81*, 6898–6926.
- (6) Romero, N. A.; Nicewicz, D. A. Organic Photoredox Catalysis. *Chem. Rev.* **2016**, *116*, 10075–10166.
- (7) (a) Kisch, H. Semiconductor Photocatalysis—Mechanistic and Synthetic Aspects. *Angew. Chem., Int. Ed.* **2013**, *52*, 812–847. (b) Kisch, H. Semiconductor Photocatalysis for Chemoselective Radical Coupling Reactions. *Acc. Chem. Res.* **2017**, *50*, 1002–1010.
- (8) Devery Iii, J. J.; Douglas, J. J.; Nguyen, J. D.; Cole, K. P.; Flowers Ii, R. A.; Stephenson, C. R. J. Ligand functionalization as a deactivation pathway in a *fac*-Ir(ppy)₃-mediated radical addition. *Chem. Sci.* **2015**, *6*, 537–541.
- (9) O'Brien, C. J.; Droge, D. G.; Jiu, A. Y.; Gandhi, S. S.; Paras, N. A.; Olson, S. H.; Conrad, J. Photoredox Cyanomethylation of Indoles: Catalyst Modification and Mechanism. *J. Org. Chem.* **2018**, *83*, 8926–8935.
- (10) Ghosh, I.; Khamrai, J.; Savateev, A.; Shlapakov, N.; Antonietti, M.; König, B. Organic semiconductor photocatalyst can bifunctionalize arenes and heteroarenes. *Science* **2019**, *365*, 360–366.
- (11) Majek, M.; Filace, F.; van Wangelin, A. J. On the mechanism of photocatalytic reactions with eosin Y. *Beilstein J. Org. Chem.* **2014**, *10*, 981–989.
- (12) Wang, X.; Maeda, K.; Thomas, A.; Takanabe, K.; Xin, G.; Carlsson, J. M.; Domen, K.; Antonietti, M. A metal-free polymeric photocatalyst for hydrogen production from water under visible light. *Nat. Mater.* **2009**, *8*, 76–80.
- (13) Wang, Y.; Wang, X.; Antonietti, M. Polymeric Graphitic Carbon Nitride as a Heterogeneous Organocatalyst: From Photochemistry to Multipurpose Catalysis to Sustainable Chemistry. *Angew. Chem., Int. Ed.* **2012**, *51*, 68–89.
- (14) Liebig, J. Über einige Stickstoff-Verbindungen. *Ann. Pharm.* **1834**, *10*, 1–47.
- (15) (a) Gisbertz, S.; Pieber, B. Heterogeneous Photocatalysis in Organic Synthesis. *ChemPhotoChem* **2020**, *4*, 456–475. (b) Mazzanti, S.; Savateev, A. Emerging Concepts in Carbon Nitride Organic Photocatalysis. *ChemPlusChem* **2020**, *85*, 2499–2517. (c) Xiao, J.; Liu, X.; Pan, L.; Shi, C.; Zhang, X.; Zou, J.-J. Heterogeneous Photocatalytic Organic Transformation Reactions Using Conjugated Polymers-Based Materials. *ACS Catal.* **2020**, *10*, 12256–12283. (d) Zhao, X.; Deng, C.; Meng, D.; Ji, H.; Chen, C.; Song, W.; Zhao, J. Nickel-Coordinated Carbon Nitride as a Metallaphotoredox Platform for the Cross-Coupling of Aryl Halides with Alcohols. *ACS Catal.* **2020**, *10*, 15178–15185. (e) Qin, Y.; Martindale, B. C. M.; Sun, R.; Rieth, A. J.; Nocera, D. G. Solar-driven tandem photoredox nickel-catalysed cross-coupling using modified carbon nitride. *Chem. Sci.* **2020**, *11*, 7456–7461. (f) Khamrai, J.; Ghosh, I.; Savateev, A.; Antonietti, M.; König, B. Photo-Ni-Dual-Catalytic C(sp²)-C(sp³) Cross-Coupling Reactions with Mesoporous Graphitic Carbon Nitride as a Heterogeneous Organic Semiconductor Photocatalyst. *ACS Catal.* **2020**, *10*, 3526–3532.
- (16) Gerwien, A.; Schildhauer, M.; Thumser, S.; Mayer, P.; Dube, H. Direct evidence for hula twist and single-bond rotation photo-products. *Nat. Commun.* **2018**, *9*, No. 2510.
- (17) Lin, J.; Pan, Z.; Wang, X. Photochemical Reduction of CO₂ by Graphitic Carbon Nitride Polymers. *ACS Sustainable Chem. Eng.* **2014**, *2*, 353–358.
- (18) Caputo, C. A.; Gross, M. A.; Lau, V. W.; Cavazza, C.; Lotsch, B. V.; Reisner, E. Photocatalytic Hydrogen Production using Polymeric Carbon Nitride with a Hydrogenase and a Bioinspired Synthetic Ni Catalyst. *Angew. Chem., Int. Ed.* **2014**, *53*, 11538–11542.
- (19) (a) Ravelli, D.; Protti, S.; Fagnoni, M. Decatungstate Anion for Photocatalyzed “Window Ledge” Reactions. *Acc. Chem. Res.* **2016**, *49*, 2232–2242. (b) Capaldo, L.; Ravelli, D. Hydrogen Atom Transfer (HAT): A Versatile Strategy for Substrate Activation in Photocatalyzed Organic Synthesis. *Eur. J. Org. Chem.* **2017**, *2017*, 2056–2071. (c) Waele, V. D.; Poizat, O.; Fagnoni, M.; Bagno, A.; Ravelli, D. Unraveling the Key Features of the Reactive State of Decatungstate Anion in Hydrogen Atom Transfer (HAT) Photocatalysis. *ACS Catal.* **2016**, *6*, 7174–7182. (d) Ide, T.; Barham, J. P.; Fujita, M.; Kawato, Y.; Egami, H.; Hamashima, Y. Regio- and chemoselective Csp³-H arylation of benzylamines by single electron transfer/hydrogen atom transfer synergistic catalysis. *Chem. Sci.* **2018**, *9*, 8453–8460.
- (20) Cai, Y.; Tang, Y.; Fan, L.; Lefebvre, Q.; Hou, H.; Rueping, M. Heterogeneous Visible-Light Photoredox Catalysis with Graphitic Carbon Nitride for α -Aminoalkyl Radical Additions, Allylations, and Heteroarylations. *ACS Catal.* **2018**, *8*, 9471–9476.
- (21) Deng, H.-P.; Fan, X.-Z.; Chen, Z.-H.; Xu, Q.-H.; Wu, J. Photoinduced Nickel-Catalyzed Chemo- and Regioselective Hydroalkylation of Internal Alkynes with Ether and Amide α -Hetero C(sp³)-H Bonds. *J. Am. Chem. Soc.* **2017**, *139*, 13579–13584.
- (22) Laudadio, G.; Deng, Y.; van der Wal, K.; Ravelli, D.; Nuño, M.; Fagnoni, M.; Guthrie, D.; Sun, Y.; Noël, T. C(sp³)-H functionaliza-

tions of light hydrocarbons using decatungstate photocatalysis in flow. *Science* **2020**, 369, 92.

(23) Perry, I. B.; Brewer, T. F.; Sarver, P. J.; Schultz, D. M.; DiRocco, D. A.; MacMillan, D. W. C. Direct arylation of strong aliphatic C–H bonds. *Nature* **2018**, 560, 70–75.

(24) Jia, P.; Li, Q.; Poh, W. C.; Jiang, H.; Liu, H.; Deng, H.; Wu, J. Light-Promoted Bromine-Radical-Mediated Selective Alkylation and Amination of Unactivated C(sp³)–H Bonds. *Chem* **2020**, 6, 1766–1776.

(25) Choi, G. J.; Zhu, Q.; Miller, D. C.; Gu, C. J.; Knowles, R. R. Catalytic alkylation of remote C–H bonds enabled by proton-coupled electron transfer. *Nature* **2016**, 539, 268–271.

(26) Chu, J. C. K.; Rovis, T. Amide-directed photoredox-catalysed C–C bond formation at unactivated sp³ C–H bonds. *Nature* **2016**, 539, 272–275.

(27) Shaw, M. H.; Shurtleff, V. W.; Terrett, J. A.; Cuthbertson, J. D.; MacMillan, D. W. C. Native functionality in triple catalytic cross-coupling: sp³ C–H bonds as latent nucleophiles. *Science* **2016**, 352, 1304–1308.

(28) (a) Hwang, S. J.; Anderson, B. L.; Powers, D. C.; Maher, A. G.; Hadt, R. G.; Nocera, D. G. Halogen Photoelimination from Monomeric Nickel(III) Complexes Enabled by the Secondary Coordination Sphere. *Organometallics* **2015**, 34, 4766–4774.

(b) Shields, B. J.; Doyle, A. G. Direct C(sp³)–H Cross Coupling Enabled by Catalytic Generation of Chlorine Radicals. *J. Am. Chem. Soc.* **2016**, 138, 12719–12722. (c) Heitz, D. R.; Tellis, J. C.; Molander, G. A. Photochemical Nickel-Catalyzed C–H Arylation: Synthetic Scope and Mechanistic Investigations. *J. Am. Chem. Soc.* **2016**, 138, 12715–12718. (d) Ackermann, L. K. G.; Martinez Alvarado, J. I.; Doyle, A. G. Direct C–C Bond Formation from Alkanes Using Ni-Photoredox Catalysis. *J. Am. Chem. Soc.* **2018**, 140, 14059–14063. (e) Kariofillis, S. K.; Shields, B. J.; Tekle-Smith, M. A.; Zacuto, M. J.; Doyle, A. G. Nickel/Photoredox-Catalyzed Methylation of (Hetero)aryl Chlorides Using Trimethyl Orthoformate as a Methyl Radical Source. *J. Am. Chem. Soc.* **2020**, 142, 7683–7689. (f) Kawasaki, T.; Ishida, N.; Murakami, M. Dehydrogenative Coupling of Benzylic and Aldehydic C–H Bonds. *J. Am. Chem. Soc.* **2020**, 142, 3366–3370. (g) Shu, X.; Huan, L.; Huang, Q.; Huo, H. Direct Enantioselective C(sp³)–H Acylation for the Synthesis of α -Amino Ketones. *J. Am. Chem. Soc.* **2020**, 142, 19058–19064.

(29) (a) Newhouse, T.; Baran, P. S. If C–H Bonds Could Talk: Selective C–H Bond Oxidation. *Angew. Chem., Int. Ed.* **2011**, 50, 3362–3374. (b) White, M. C. Adding Aliphatic C–H Bond Oxidations to Synthesis. *Science* **2012**, 335, 807–809.

(30) (a) Hansen, E. C.; Li, C.; Yang, S.; Pedro, D.; Weix, D. J. Coupling of Challenging Heteroaryl Halides with Alkyl Halides via Nickel-Catalyzed Cross-Electrophile Coupling. *J. Org. Chem.* **2017**, 82, 7085–7092. (b) Shen, Y.; Gu, Y.; Martin, R. sp³ C–H Arylation and Alkylation Enabled by the Synergy of Triplet Excited Ketones and Nickel Catalysts. *J. Am. Chem. Soc.* **2018**, 140, 12200–12209. (c) Milligan, J. A.; Phelan, J. P.; Badir, S. O.; Molander, G. A. Alkyl Carbon–Carbon Bond Formation by Nickel/Photoredox Cross-Coupling. *Angew. Chem., Int. Ed.* **2019**, 58, 6152–6163. (d) Wang, D.-H.; Hao, X.-S.; Wu, D.-F.; Yu, J.-Q. Palladium-Catalyzed Oxidation of Boc-Protected N-Methylamines with IOAc as the Oxidant: A Boc-Directed sp³ C–H Bond Activation. *Org. Lett.* **2006**, 8, 3387–3390. (e) Jain, P.; Verma, P.; Xia, G.; Yu, J.-Q. Enantioselective amine α -functionalization via palladium-catalysed C–H arylation of thioamides. *Nat. Chem.* **2017**, 9, 140–144.

(31) (a) Kavarnos, G. J.; Turro, N. J. Photosensitization by reversible electron transfer: theories, experimental evidence, and examples. *Chem. Rev.* **1986**, 86, 401–449. (b) Strieth-Kalthoff, F.; James, M. J.; Teders, M.; Pitzer, L.; Glorius, F. Energy transfer catalysis mediated by visible light: principles, applications, directions. *Chem. Soc. Rev.* **2018**, 47, 7190–7202.

(32) Beyreuther, B. K.; Freitag, J.; Heers, C.; Krebsfänger, N.; Scharfenecker, U.; Stöhr, T. Lacosamide: A Review of Preclinical Properties. *CNS Drug Rev.* **2007**, 13, 21–42.

(33) Cambié, D.; Bottecchia, C.; Straathof, N. J. W.; Hessel, V.; Noël, T. Applications of Continuous-Flow Photochemistry in Organic Synthesis, Material Science, and Water Treatment. *Chem. Rev.* **2016**, 116, 10276–10341.

(34) Rosso, C.; Gisbertz, S.; Williams, J. D.; Gemoets, H. P. L.; Debrouwer, W.; Pieber, B.; Kappe, C. O. An oscillatory plug flow photoreactor facilitates semi-heterogeneous dual nickel/carbon nitride photocatalytic C–N couplings. *React. Chem. Eng.* **2020**, 5, 597–604.

(35) Barry, J. T.; Berg, D. J.; Tyler, D. R. Radical Cage Effects: Comparison of Solvent Bulk Viscosity and Microviscosity in Predicting the Recombination Efficiencies of Radical Cage Pairs. *J. Am. Chem. Soc.* **2016**, 138, 9389–9392.

(36) Rohe, S.; Morris, A. O.; McCallum, T.; Barriault, L. Hydrogen Atom Transfer Reactions via Photoredox Catalyzed Chlorine Atom Generation. *Angew. Chem., Int. Ed.* **2018**, 57, 15664–15669.

(37) Echeverria, V.; Zeitlin, R. Cotinine: a potential new therapeutic agent against Alzheimer's disease. *CNS Neurosci. Ther.* **2012**, 18, 517–523.

(38) Barham, J. P.; John, M. P.; Murphy, J. A. Contra-thermodynamic Hydrogen Atom Abstraction in the Selective C–H Functionalization of Trialkylamine N-CH₃ Groups. *J. Am. Chem. Soc.* **2016**, 138, 15482–15487.

(39) Gisbertz, S.; Reischauer, S.; Pieber, B. Overcoming limitations in dual photoredox/nickel-catalysed C–N cross-couplings due to catalyst deactivation. *Nat. Catal.* **2020**, 3, 611–620.

(40) Pieber, B.; Malik, J. A.; Cavedon, C.; Gisbertz, S.; Savateev, A.; Cruz, D.; Heil, T.; Zhang, G.; Seeberger, P. H. Semi-heterogeneous Dual Nickel/Photocatalysis using Carbon Nitrides: Esterification of Carboxylic Acids with Aryl Halides. *Angew. Chem., Int. Ed.* **2019**, 58, 9575–9580.

(41) (a) Diccianni, J. B.; Diao, T. Mechanisms of Nickel-Catalyzed Cross-Coupling Reactions. *Trends Chem.* **2019**, 1, 830–844. (b) Ting, S. I.; Garakyaraghi, S.; Taliaferro, C. M.; Shields, B. J.; Scholes, G. D.; Castellano, F. N.; Doyle, A. G. 3d-d Excited States of Ni(II) Complexes Relevant to Photoredox Catalysis: Spectroscopic Identification and Mechanistic Implications. *J. Am. Chem. Soc.* **2020**, 142, 5800–5810. (c) Maity, B.; Zhu, C.; Yue, H.; Huang, L.; Harb, M.; Minenkov, Y.; Rueping, M.; Cavallo, L. Mechanistic Insight into the Photoredox-Nickel-HAT Triple Catalyzed Arylation and Alkylation of α -Amino Csp³–H Bonds. *J. Am. Chem. Soc.* **2020**, 142, 16942–16952.

(42) Savateev, A.; Tarakina, N. V.; Strauss, V.; Hussain, T.; ten Brummelhuis, K.; Sánchez Vadillo, J. M.; Markushyna, Y.; Mazzanti, S.; Tyutyunnik, A. P.; Walczak, R.; Oschatz, M.; Guldi, D. M.; Karton, A.; Antonietti, M. Potassium Poly(Heptazine Imide): Transition Metal-Free Solid-State Triplet Sensitizer in Cascade Energy Transfer and [3+2]-cycloadditions. *Angew. Chem., Int. Ed.* **2020**, 59, 15061–15068.

(43) Malik, J. A.; Madani, A.; Pieber, B.; Seeberger, P. H. Evidence for Photocatalyst Involvement in Oxidative Additions of Nickel-Catalyzed Carboxylate O-Arylations. *J. Am. Chem. Soc.* **2020**, 142, 11042–11049.

(44) (a) Welin, E. R.; Le, C.; Arias-Rotondo, D. M.; McCusker, J. K.; MacMillan, D. W. C. Photosensitized, energy transfer-mediated organometallic catalysis through electronically excited nickel(II). *Science* **2017**, 355, 380–385. (b) Sun, R.; Qin, Y.; Ruccolo, S.; Schnedermann, C.; Costentin, C.; Daniel, G. N. Elucidation of a Redox-Mediated Reaction Cycle for Nickel-Catalyzed Cross Coupling. *J. Am. Chem. Soc.* **2019**, 141, 89–93.